Viral DNA Replication-Dependent DNA Damage Response Activation during BK Polyomavirus Infection

Brandy Verhalen,[a] Joshua L. Justice,[a] Michael J. Imperiale,[b] Mengxi Jiang[a]

Department of Microbiology, University of Alabama at Birmingham, Birmingham, Alabama, USA[a]; Department of Microbiology and Immunology and Comprehensive Cancer Center, University of Michigan Medical School, Ann Arbor, Michigan, USA[b]

ABSTRACT

BK polyomavirus (BKPyV) reactivation is associated with severe human disease in kidney and bone marrow transplant patients. The interplay between viral and host factors that regulates the productive infection process remains poorly understood. We have previously reported that the cellular DNA damage response (DDR) is activated upon lytic BKPyV infection and that its activation is required for optimal viral replication in primary kidney epithelial cells. In this report, we set out to determine what viral components are responsible for activating the two major phosphatidylinositol 3-kinase-like kinases (PI3KKs) involved in the DDR: ataxia telangiectasia mutated (ATM) kinase and ATM and Rad3-related (ATR) kinase. Using a combination of UV treatment, lentivirus transduction, and mutant virus infection experiments, our results demonstrate that neither the input virus nor the expression of large T antigen (TAg) alone is sufficient to trigger the activation of ATM or ATR in our primary culture model. Instead, our data suggest that the activation of both the ATM- and ATR-mediated DDR pathways is linked to viral DNA replication. Intriguingly, a TAg mutant virus that is unable to activate the DDR causes substantial host DNA damage. Our study provides insight into how DDRs are activated by polyomaviruses in primary cells with intact cell cycle checkpoints and how the activation might be linked to the maintenance of host genome stability.

IMPORTANCE

Polyomaviruses are opportunistic pathogens that are associated with several human diseases under immunosuppressed conditions. BK polyomavirus (BKPyV) affects mostly kidney and bone marrow transplant patients. The detailed replication mechanism of these viruses remains to be determined. We have previously reported that BKPyV activates the host DNA damage response (DDR), a response normally used by the host cell to combat genotoxic stress, to aid its own replication. In this study, we identified that the trigger for DDR activation is viral replication. Furthermore, we show that the virus is able to cause host DNA damage in the absence of viral replication and DDR activation. These results suggest an intricate relationship between viral replication, DDR activation, and host genome instability.

The BK polyomavirus (BKPyV) is a ubiquitous opportunistic human pathogen which causes severe disease in immunocompromised patients (1). BKPyV is thought to be acquired through the respiratory route during early childhood, and by adulthood, up to 90% of the general population becomes seropositive (2). Following primary exposure, the virus establishes a lifelong, subclinical, persistent infection in the genitourinary tract. BKPyV can reactivate from the persistent state under immunosuppressed conditions, most commonly in kidney transplant patients, resulting in viral shedding in urine or blood and, ultimately, polyomavirus-associated nephropathy, a significant cause of renal dysfunction (3). There are no FDA-approved therapies for BKPyV infection, and the usual treatment is to reduce immunosuppression to allow the immune system to regain control over BKPyV, which increases the likelihood of transplant rejection.

BKPyV is a small (40 to 45 nm in diameter), nonenveloped virus that contains an ~5-kb circular double-stranded DNA genome. Following entry, the viral DNA genome is delivered into the nucleus, where replication occurs. The mechanisms of BKPyV replication have largely been extrapolated from work on simian virus 40 (SV40), a closely related polyomavirus. Because of its small genome size and, hence, limited coding capacity, polyomavirus replication relies heavily on the host replication machinery. In particular, large T antigen (TAg), a multifunctional protein, orchestrates the viral replication cycle by recruiting replication

protein A (RPA), DNA polymerase alpha-primase, and topoisomerase I to replicate viral DNA (4). Over the years, SV40 DNA replication has been pursued as a model system to understand mammalian chromosome replication, and the bidirectional replication mechanism is considered a common feature between viral and host DNA replication (5).

One of the emerging concepts in the polyomavirus field is that these viruses are able to hijack and engage cellular DNA damage response (DDR) components during viral replication. DDR signaling cascades are initiated to combat a diverse array of deleterious assaults on the host genome, which allows the cells to maintain chromosome integrity. In the past few years, both the ataxia telangiectasia mutated (ATM) kinase and the ATM and Rad3-related (ATR) kinase-medi-

ated DDRs have been implicated in a number of polyomavirus infections, including BKPyV, SV40, JC polyomavirus (JCPyV), murine polyomavirus (mPyV), and Merkel cell polyomavirus (MCPyV) infections (6–11). ATM is a major responder to double-stranded breaks (DSBs) resulting from conditions such as ionizing irradiation (IR). ATR is activated by single-stranded DNA lesions resulting from conditions such as replication stress. More specifically, both ATM and ATR have been shown to be important to maintain replication fork integrity by resolving replication intermediates and replication-induced stress and breaks (6). DDR activation-associated cell cycle G$_2$ arrest has also been suggested to be another main reason why polyomaviruses need to activate the DDR (9, 10). Finally, there is evidence that ATM can contribute to SV40 DNA replication by directly phosphorylating TAg (12).

Using a primary human renal proximal tubule epithelial (RPTE) cell culture model (13), we have previously shown that BKPyV is able to activate both the ATM- and the ATR-mediated DDRs and that both pathways function to ensure optimal viral replication and infectious progeny production (14). In addition, we have demonstrated that in the absence of either ATM or ATR, there is an accumulation of host DNA damage in BKPyV-infected cells, as evidenced by the appearance of abnormal nuclei and a dramatic increase in the number of damaged metaphase chromosomes (14). In this study, we aimed to further understand how the DDRs are activated by BKPyV and how the activation might be tied to the host genome stability. Our results suggest that viral DNA replication is the trigger for both ATM- and ATR-mediated DDR activation and that the activated DDR is able to protect cells from BKPyV-induced host DNA damage.

MATERIALS AND METHODS

Cell culture, viruses, infection, and transduction. RPTE cells (Lonza) were maintained in renal epithelial cell growth medium (REGM) as previously described (15). Vero cells and 293TT cells were maintained as previously described (16, 17). All cells were grown at 37°C with 5% CO$_2$ in a humidified incubator.

BKPyV (Dunlop) was grown in Vero cells, and the viral titer was determined using an infectious unit (IU) assay as previously described (16). For infections, RPTE cells were prechilled for 15 min at 4°C. BKPyV diluted in REGM was added to the cells at the multiplicities of infection (MOIs) indicated below and incubated for 1 h at 4°C. Infection was initiated by removing the viral inoculum, feeding with prewarmed REGM, and transferring the cells to the temperatures indicated below for the indicated durations for each experiment. For UV inactivation, virus was treated with 4 J of UV light using a UV Stratalinker (Stratagene). Total cell proteins and viral lysates were harvested as previously described (15). Lentivirus was produced in 293T cells using transfection conditions as previously described (18). For lentivirus transduction, RPTE cells were transduced with control lentivirus or lentivirus expressing BKPyV TAg (lenti-TAg) in the presence of 8 μg/ml Polybrene (each well of a 6-well plate received 60 μl concentrated virus harvested from a 1- by 10-cm dish) for 6 h at 37°C. The amount of lentivirus used was determined such that similar levels of TAg (by Western blotting) were produced from lenti-TAg-transduced cells and cells that were infected with BKPyV at an MOI of 0.01 IU/cell at 37°C. The viral inoculum was replaced with fresh REGM, and protein lysates from both infected and transduced cells were harvested 3 days after BKPyV infection and lentivirus transduction, respectively.

Site-directed mutagenesis. The following mutagenic primers were synthesized, purified by high-performance liquid chromatography (HPLC), and used to introduce mutations into TAg on the pBR322-Dunlop backbone: for the R359K mutation (a change of arginine to lysine at position 359), MJ#68 (5′ CTGTTAGCATTTCTTCCTTGGTCATATGA

AGGGTATCTAC 3′) and MJ#69 (5′ GTAGATACCCTTCATATGACCA AGGAAGAAATGCTAACAG 3′), and for the TAg D501A mutation, MJ#74 (5′ GACAGTTTGAGAGCCTATTTAGATGGAAGTG 3′) and MJ#75 (5′ CACTTCCATCTAAATAGGCTCTCAAACTGTC 3′). Mutagenesis was performed using the primer pairs at 125 ng each, 100 ng of pBR322-Dunlop as the template, 1 mM deoxynucleoside triphosphates (dNTPs), and 1.25 U PfuUltra DNA polymerase (Agilent Technologies) in 25-μl reaction mixtures. The following PCR program was used: 3 min at 95°C, 18 cycles of 95°C for 15 s, and annealing and extension at 65°C or 68°C for 16.5 min. The mutations were confirmed by sequencing.

Growth of mutant viruses. To grow the TAg R359K mutant virus, the viral genome was excised from the pBR322 backbone, religated, and transfected into RPTE cells as previously described (15). Cells were maintained at 32°C (permissive temperature), and the resulting crude lysate titers were determined using the IU assay performed at 32°C (16). For the TAg D501A mutant virus, the mutant viral genome was processed similarly and transfected into 293TT cells. Viral lysates were harvested, and viral titers were determined as previously described (19).

Western blotting. Total cell proteins were harvested, quantified, and immunoblotted as previously described (16). Antibodies were used at previously described concentrations (14). For all the experiments for which representative results are shown in the figures, multiple gels were run in each independent experiment in order to cover all the proteins that were probed.

Immunofluorescence microscopy. At different times postinfection (p.i.), RPTE cells were fixed and immunostained as previously described (18). For standard fluorescence microscopy, samples were examined using an Olympus IX81 microscope with a Plan 40×/0.75 objective and processed using CellSens Dimension software. To quantify aberrant nuclei morphology, at least 80 nuclei were scored under each condition per replicate.

Real-time PCR. To quantify viral DNA replication in cells, low-molecular-weight DNA was isolated using a modified Hirt protocol (18). Real-time PCRs were performed, and data were analyzed as previously described (18). Replicated DNA at various time points postinfection was normalized to input DNA harvested 1 day p.i. using a previously described cycle threshold (ΔC_T) method (19).

Comet assay. To detect DNA damage in RPTE cells, an alkaline comet assay was used after infection with wild-type (WT) or replication-deficient BKPyV. Three days postinfection, cells were trypsinized and comet assays were performed using the CometAssay kit (Trevigen) according to the manufacturer's instructions. The slides were imaged with an Olympus IX81 microscope with a Plan 10×/0.3 objective and analyzed using Open-Comet software (http://www.opencomet.org/). Three replicates were performed, with at least 50 events scored per replicate per condition.

RESULTS

Input BKPyV is not sufficient to activate the DDR. For certain DNA viruses, such as adenovirus, input viral DNA is recognized by the cells as damaged DNA and triggers the DDR (20). We began our studies by examining whether input BKPyV virus is able to activate the DDR. To test this, we treated the viral inoculum with UV light and used the UV-inactivated virus to infect RPTE cells. Under the conditions we used, UV treatment is able to reduce the infectivity of the virus, as shown by a significant decrease in both TAg expression (Fig. 1A) and the viral DNA level (Fig. 1B) at 3 days p.i. In addition, compared with the result for untreated virus, no increase in VP1 was detected by Western blotting at 3 days p.i.: the VP1 at 1 day p.i. is from the infection inoculum (16). Having established that UV treatment reduces replication, we then probed the whole-cell lysates for markers of DDR activation, including ATM-pS1981 for ATM activation (21) and Chk1-pS317 for ATR activation (22). Unlike the cells that were infected with untreated BKPyV, RPTE cells that were infected with UV-inacti-
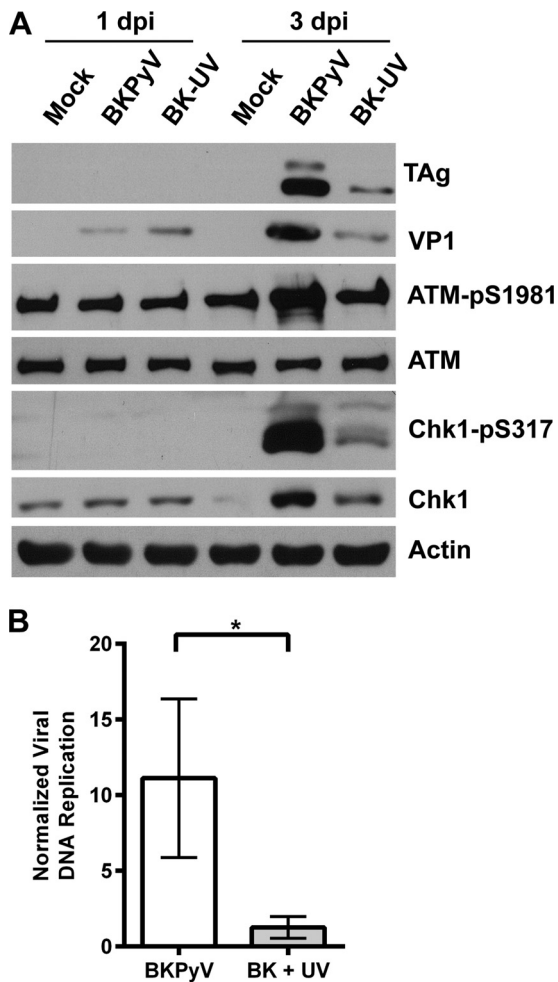
FIG 1 UV treatment of viral inoculum abolishes DDR activation. (A) BKPyV crude lysates were either untreated or treated with 4 J of UV prior to infection of RPTE cells at an MOI of 0.5 IU/cell. Total proteins were harvested at 1 day p.i. and 3 days p.i. and probed for the indicated proteins by Western blotting. Shown are representative blots from three independent experiments. (B) BKPyV DNA was quantified by real-time PCR. Replicated DNA (3 days p.i.) was normalized to input DNA (1 day p.i.). Combined results from three independent experiments done in triplicates are shown. The error bars are the standard deviation (SD) values. *, $P < 0.05$ (all statistical analyses in this study were performed using a two-tailed and unpaired Student's t test).

prediction of BKPyV TAg based on the known SV40 TAg structure also revealed that this conserved arginine is present at similar positions in both structures (Fig. 3A). We introduced the same mutation (R359K) into the BKPyV genome and grew the virus at the permissive temperature, 32°C. When we infected cells with this mutant virus at 32°C, the virus was able to replicate, albeit approximately 1 log less than the wild type (WT) (Fig. 3B). However, when we performed the infection at the nonpermissive temperature, 39°C, TAg became unstable and was rapidly degraded (Fig. 3C), and therefore, the virus was unable to replicate its DNA (Fig. 3B). This provided us with a system to determine whether the input virus is sufficient to trigger the DDR at the nonpermissive temperature, since the mutant virus has no known defect in virus entry. When we probed the whole-cell lysates for DDR activation markers, we observed that at the nonpermissive temperature, the ability of the mutant virus to activate the ATM-mediated DDR is greatly reduced compared with that of the WT virus (Fig. 3C). Similar to the UV treatment experiment, ATR activation was also diminished, as evidenced by a decreased induction of Chk1-pS317 compared with its induction by the WT. This corroborates that the input virus alone is unable to activate the DDR at the same level as is observed in wild-type virus infection.

TAg expression alone is insufficient to activate the ATR-mediated DDR. For SV40, JCPyV, and MCPyV, the presence of TAg alone is sufficient to activate the DDR (10, 25, 26). To determine whether this is also the case for BKPyV in our primary cells, we transduced RPTE cells with a lentivirus expressing BKPyV TAg (lenti-TAg) (18) and compared DDR activation between lentivirus-transduced cells and BKPyV-infected cells (Fig. 4). TAg expression alone stabilized p53, as expected. Transduction with an empty lentivirus control increased ATM-pS1981; therefore, we cannot conclude whether TAg expression was able to activate the ATM-mediated DDR. TAg expression also increased the level of Chk1; however, the level of Chk1-pS317 was minimally increased compared with that in untransduced cells or cells transduced with empty lentivirus. In contrast, in cells that were infected with BKPyV at a low MOI (0.01 IU/cell), even though the TAg level was similar to that in the lenti-TAg-transduced cells, there was a strong upregulation of both ATM-pS1981 and Chk1-pS317 (Fig. 4). These results indicate that BKPyV TAg alone is not sufficient to fully activate the ATR-mediated DDR. Instead, either viral DNA replication or other viral components seem to contribute to DDR activation.

A DNA replication-deficient mutant virus is unable to activate the DDR. To examine the relationship between viral DNA replication and DDR activation, we created a viral DNA replication mutant virus based on another homologous SV40 mutant TAg (27). The D499A mutation in SV40 TAg (D501A in BKPyV) (Fig. 2 and 5A) affects the ability of TAg to unwind the origin but retains other functions, such as origin binding, double hexamer formation, and ATP hydrolysis. We introduced this mutation into the BKPyV genome and grew the virus in 293TT cells, a cell line that can complement BKPyV TAg mutations due to the expression of high levels of SV40 TAg (17, 28). We confirmed that this mutant virus is replication deficient in RPTE cells using real-time PCR to quantify viral DNA (Fig. 5B). When we infected RPTE cells with equal MOIs of the wild-type and mutant virus for 3 days, Western blotting revealed that the level of TAg present was similar to the level in the cells with the wild-type virus infection and that TAg was able to stabilize p53 (Fig. 5C). Despite this, the mutant

vated BKPyV no longer contained elevated levels of ATM-pS1981 compared with the level in the mock control cells (Fig. 1A). There was a slight increase in Chk1-pS317 in cells treated with the UV-inactivated virus compared to the level in the mock control cells, but the induction was greatly attenuated compared with the results for the untreated virus. These data suggest that the input BKPyV might be able to induce a mild ATR activation but is unable to activate the full DDR during infection.

Since UV-treated BKPyV virions may be blocked at the capsid uncoating stage and, therefore, unable to enter the nucleus, we decided to use another method to confirm that the input virus is not sufficient to activate the DDR. Previously, a temperature-sensitive mutant of SV40 was isolated that contains an R-to-K mutation at residue 357 in SV40 TAg (23). This residue is present in the leucine zipper region of TAg that overlaps the Zn finger (24), and it is conserved in BKPyV TAg at position 359 (Fig. 2). Structural

J domain

```
           J domain
SV40   MDKVLNREESLQLMDLLGLERSAWGNIPLMRKAYLKKCKEFHPDKGGDEEKMKKMNTLYK 60
BK     MDKVLNREESMELMDLLGLERAAWGNLPLMRKAYLRKCKEFHPDKGGDEDKMKRMNTLYK 60

                                                 LXCXE
SV40   KMEDGVKYAHQPDFGGFWDATEIPTYGTDEWEQWWNAFNE---ENLFCSEEMPSSDDEAT 117
BK     KMEQDVKVAHQPDFG-TWSSSEVPTYGTEEWESWWSSFNEKWDEDLFCHEDMFASDEEAT 119

SV40   ADSQHSTPPKKKRKVEDPKDFPSELLSFLSHAVFSNRTLACFAIYTTKEKAALLYKKIME 177
BK     ADSQHSTPPKKKRKVEDPKDFPSDLHQFLSQAVFSNRTLACFAVYTTKEKAQILYKKLME 179

                            OBD
SV40   KYSVTFISRHNSYNHNILFFLTPHRHRVSAINNYAQKLCTFSFLICKGVNKEYLMYSALT 237
BK     KYSVTFISRHMCAGHNIIFFLTPHRHRVSAINNFCQKLCTFSFLICKGVNKEYLLYSALT 239

SV40   RDPFSVIEESLPGGLKEHDFNPEEAEETKQVSWKLVTEYAMETKCDDVLLLLGMYLEFQY 297
BK     RDPYHTIEESIQGGLKEHDFSPEEPEETKQVSWKLITEYAVETKCEDVFLLLGMYLEFQY 299

                          Zn finger
SV40   SFEMCLKCIKKEQPSHYKYHEKHYANAAIFADSKNQKTICQQAVDTVLAKKRVDSLQLTR 357
BK     NVEECKKCQKKDQPYHFKYHEKHFANAIIFAESKNQKSICQQAVDTVLAKKRVDTLHMTR 359

SV40   EQMLTNRFNDLLDRMDIMFGSTGSADIEEWMAGVAWLHCLLPKMDSVVYDFLKCMVYNIP 417
BK     EEMLTERFNHILDKMDLIFGAHGNAVLEQYMAGVAWLHCLLPKMDSVIFDFLHCIVFNVP 419

                         ATPase
SV40   KKRYWLFKGPIDSGKTTLAAALLELCGGKALNVNLPLDRLNFELGVAIDQFLVVFEDVKG 477
BK     KRRYWLFKGPIDSGKTTLAAGLLDLCGGKALNVNLPMERLTFELGVAIDQYMVVFEDVKG 479

SV40   TGGESRDLPSGQGINNLDNLRDYLDGSVKVNLEKKHLNKRTQIFPPGIVTMNEYSVPKTL 537
BK     TGAESKDLPSGHGINNLDSLRDYLDGSVKVNLEKKHLNKRTQIFPPGLVTMNEYPVPKTL 539

SV40   QARFVKQIDFRPKDYLKHCLERSEFLLEKRIIQSGIALLLMLIWYRPVAEFAQSIQSRIV 597
BK     QARFVRQIDFRPKIYLRKSLQNSEFLLEKRILQSGMTLLLLLIWFRPVADFATDIQSRIV 599

SV40   EWKERLDKEFSLSVYQKMKFNVAMGIGVLDWLRNSDDDDEDSQENADKNEDGGEKNMEDS 657
BK     EWKERLDSEISMYTFSRMKYNICMGKCILDITREEDSETEDS----------GHGSSTES 649

SV40   GHETGIDSQSQGSFQAPQSSQSVHDHNQPYHICRGFTCFKKPPTPPPEPET 708
BK     --QSQCSSQVSDTSAPAEDSQRSDPHSQELHLCKGFQCFKRPKTPPPPK--- 695
```

FIG 2 SV40 and BKPyV TAg alignment. Several conserved domains and motifs, including the J domain, the LXCXE motif, the origin binding domain (OBD), the Zn finger, and the ATPase domain, are highlighted in different colors. The two residues that were mutated in this study (BKPyV R359K and D501A) are boxed in red.

virus was unable to activate either the ATM- or ATR-mediated DDR, as shown by a lack of upregulation of ATM-pS1981 or Chk1-pS317. These data suggest that the DDR activation caused by BKPyV infection is linked to viral DNA replication.

TAg D501A mutant virus infection causes host DNA damage. Interestingly, we observed the appearance of aberrant nuclei when we infected cells with the TAg D501A mutant. At 3 days p.i., DAPI (4′,6-diamidino-2-phenylindole)-stained nuclei appeared to have uneven edges or were fragmented, as opposed to the normal oval shape in wild-type virus-infected cells (Fig. 6A). Similarly abnormal TAg immunostaining was also observed. Relative to the numbers in cells infected with the wild-type virus, there were significantly higher numbers of these abnormal nuclei in the mutant-infected cells (Fig. 6B and C).

Previously, we have also observed an abnormal nuclear phenotype in BKPyV-infected cells treated with ATM or ATR small interfering RNAs (siRNAs), which correlated with increased host DNA damage (14). To assess whether the abnormal nuclei we observed during infection of the TAg D501A mutant virus were indicative of host DNA damage, we applied an alkaline comet assay to determine the levels of host DNA damage in cells (Fig. 7). We observed very little DNA damage in either the mock- or wild-type BKPyV-infected cells. In contrast, infection with the TAg D501A virus resulted in a larger proportion of the cells with a comet tail phenotype (Fig. 7A) and a statistically significant in-

crease in the percentage of DNA in the comet tail (Fig. 7B) compared with the results for the wild-type control. Thus, this mutant virus is unable to activate the DDR upon infection but can cause host DNA damage, which is absent during normal viral infection.

DISCUSSION

In this study, we performed a series of experiments to identify viral components that are crucial to trigger DDR activation during BKPyV infection. This is an important question, as it has been shown for several polyomaviruses that inhibition of DDR activation can result in decreased viral infection (7, 9–11, 14). Our results indicated that, unlike some DNA viruses, the input BKPyV virus is incapable of activating a strong ATM- or ATR-mediated DDR during the initial infection (Fig. 1 and 3). Instead, the fact that a replication-deficient mutant virus is unable to activate the DDR suggests that activation is linked to the viral DNA replication. Interestingly, this mutant virus infection leads to an accumulation of host DNA damage, which is not observed with wild-type infection (Fig. 6 and 7). Previously, we proposed a model for DDR activation and maintenance of host genome stability during BKPyV infection in which a functional DDR was required both directly and indirectly for viral replication (14). The results in this report allow us to add to the model the fact that it is viral replication that results in both ATM- and ATR-mediated DDR activa-
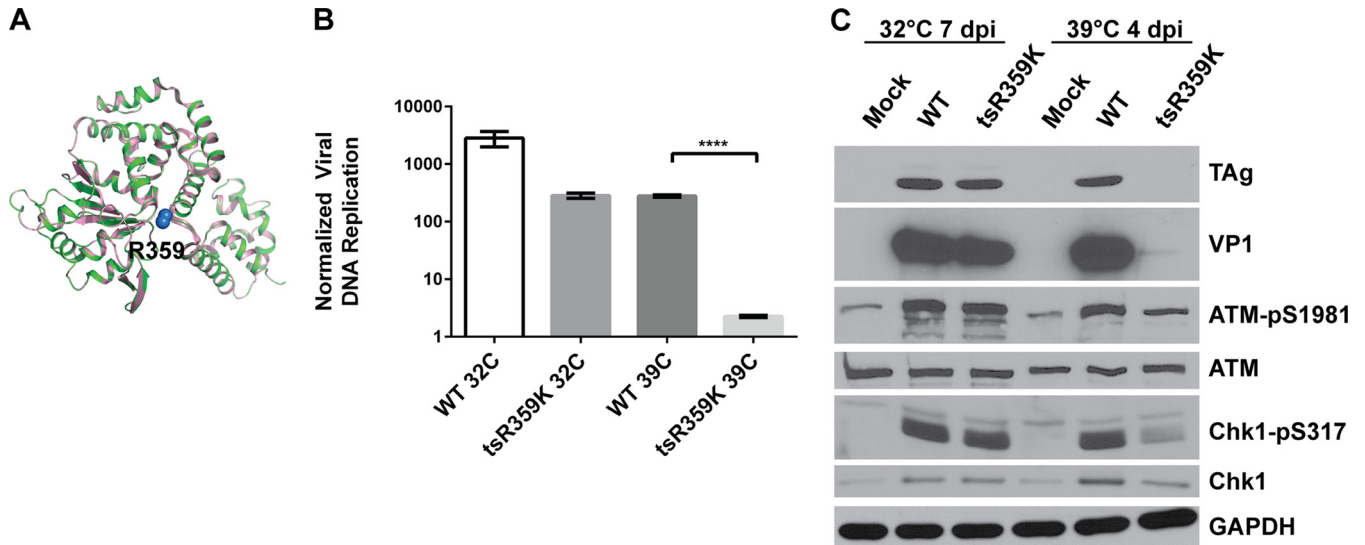
FIG 3 The temperature-sensitive R359K (tsR359K) TAg mutant virus is unable to fully activate the DDR at the nonpermissive temperature. (A) Alignment of SV40 (PDB ID 1SVO, pink) and BKPyV TAg (predicted using SWISS-MODEL, green) ribbon structures, with the Cβ and the Cγ atoms of the R359 residue of BKPyV TAg depicted as blue spheres. Alignment was done in Pymol. (B) RPTE cells were infected with WT or tsR359K mutant BKPyV at an MOI of 0.05 IU/cell. Low-molecular-weight DNA was harvested at 1 day p.i. (for both 32°C and 39°C), 7 days p.i. (32°C), and 4 days p.i. (39°C). The later time point was used for the mutant because replication is slower at the lower temperature (data not shown). BKPyV DNA was quantified by quantitative PCR in triplicates. Replicated DNA (7 days p.i. at 32°C or 4 days p.i. at 39°C) was normalized to input DNA (1 day p.i.). Data shown are from one experiment that is representative of three independent experiments. The error bars show the SD values. ****, $P < 0.0001$. (C) Total proteins from cells grown at the different temperatures were harvested at the indicated times postinfection and probed for the indicated proteins by Western blotting. The blots shown are representative of at least three independent experiments.

tion, and this activated DDR, in turn, can suppress host DNA genome damage caused by BKPyV (Fig. 8).

Intriguingly, we did not observe a strong activation of the ATR-mediated DDR in the presence of TAg expression alone
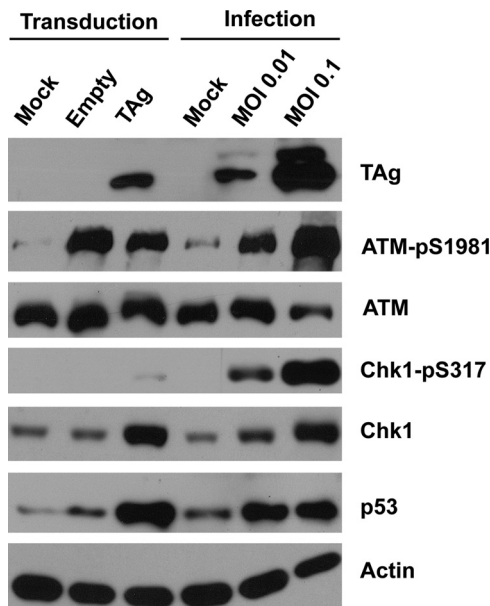

FIG 4 TAg alone is not sufficient to fully activate ATR-mediated DDR. RPTE cells were either transduced with empty or TAg-expressing lentivirus or infected with BKPyV at the designated MOIs for 3 days. Total proteins from cells grown at the different temperatures were harvested at the indicated times postinfection and probed for the indicated proteins by Western blotting. The blots shown are representative of three independent experiments.

(Fig. 4). This result is different from what was reported for JCPyV, MCPyV, and SV40 (10, 25, 26). Although it is possible that this discrepancy is due to the nature of BKPyV TAg, we think a more likely explanation is the difference in cell types. Most of the previous studies were performed using immortalized cell lines, whereas we are examining the DDR activation in primary cells in which there are intact cell cycle checkpoints. This difference between cell lines and primary cells with regard to DDR activation and DNA repair pathway choice is not unprecedented. For example, studies in many cancer cells led to the general belief that homologous recombination (HR) is the preferred repair pathway in S, G$_2$, and M phases; however, a recent study in normal cells reveals that HR activity declines, whereas the nonhomologous end-joining repair pathway is more dominant in G$_2$ (29). Another possibility is that TAg expression levels might be different between lentivirus-transduced cells and BKPyV-infected cells. Unfortunately, we cannot assess TAg levels on a single-cell level using flow cytometry or immunofluorescence microscopy because lenti-TAg produces a high level of truncTAg (a TAg splicing variant [30]), which is also recognized by the pAb416 antibody that we use for TAg staining.

Similarly, we also demonstrated differences in host DNA damage induction by BKPyV compared to DNA damage induction by other polyomaviruses. For SV40 or MCPyV, TAg expression alone can induce DNA damage, as visualized by the comet assay (26, 31). In contrast, we did not observe any host DNA damage under normal infection conditions (Fig. 7). Only when ATM or ATR was inhibited (14) or viral DNA replication was blocked (Fig. 6 and 7) did we observe severe host DNA damage during infection. This suggests that BKPyV is capable of causing host damage, possibly through TAg, but that this damage is likely repaired by the activated DDRs during normal replication. Alternatively, it is possible that BKPyV infection results in host replication stress and mitotic
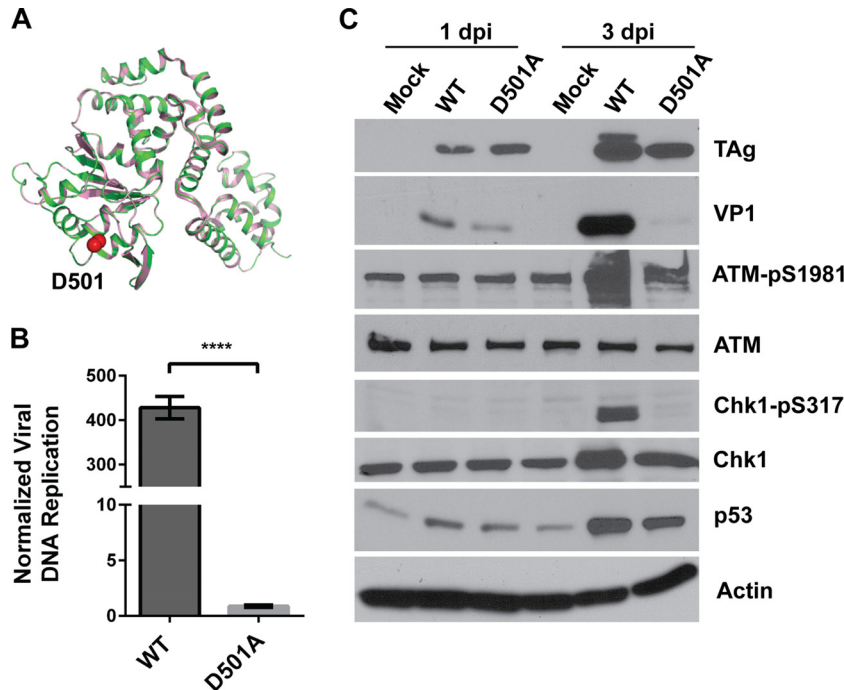
FIG 5 The replication-deficient TAg D501A mutant virus is unable to activate the DDR. (A) Alignment of SV40 and BKPyV TAg cartoon structures as described in the legend to Fig. 3A, with the Cβ and the Cγ atoms of the D501 residue of BKPyV TAg depicted as red spheres. (B) RPTE cells were infected with wild-type or TAg D501A mutant BKPyV at an MOI of 0.5 IU/cell. Low-molecular-weight DNA was harvested at 1 day p.i. and 3 days p.i., and BKPyV DNA was quantified by quantitative PCR in triplicates. Replicated DNA (3 days p.i.) was normalized to input DNA (1 day p.i.). Data shown are for one experiment that is representative of three independent experiments. The error bars show the SD values. ****, $P < 0.0001$. (C) Total proteins were harvested at 1 day p.i. and 3 days p.i. and probed for the indicated proteins by Western blotting. The blots shown are representative of at least three independent experiments.

dysfunction, similar to what has been reported for SV40 TAg (32). During normal infection, however, the damage is not apparent because the cells are arrested in G_2 (14). Only when the cell cycle arrest caused by ATM or ATR activation is removed and the cells enter mitosis does this damage become evident. The latter may provide another reason for polyomaviruses in general to activate the DDR and arrest the cell cycle in G_2 phase. Not only do these viruses need to hijack the DDR machinery to perhaps resolve rep-
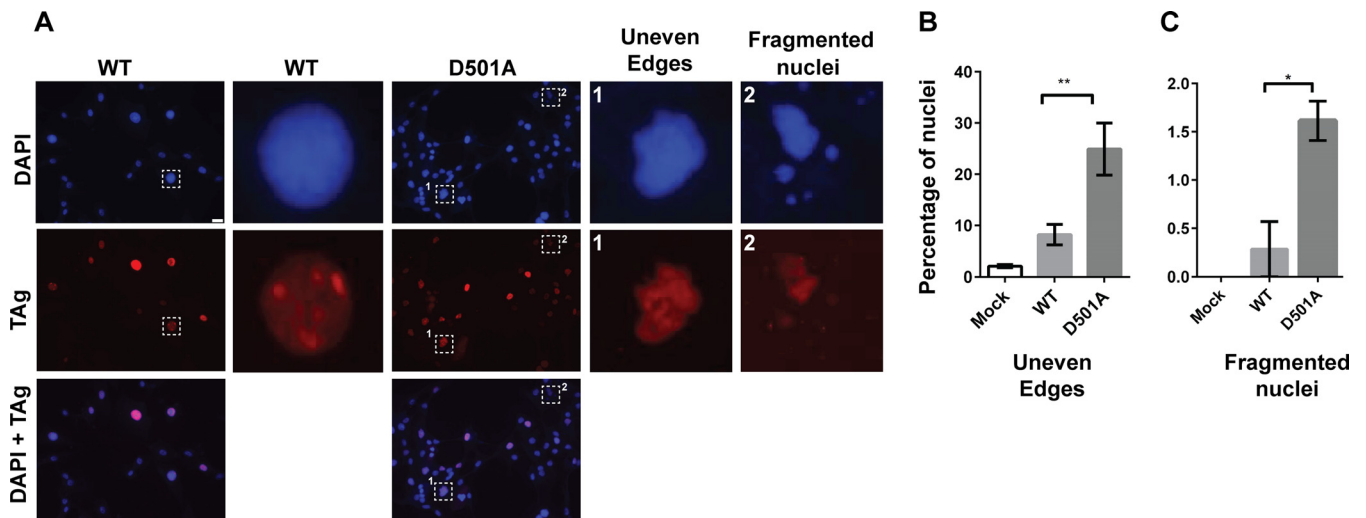

FIG 6 TAg D501A mutant virus infection results in aberrant DAPI and TAg staining patterns. (A) Cells were infected with WT or TAg D501A mutant BKPyV as described in the legend to Fig. 5. Cells were fixed at 3 days p.i. and stained with DAPI (blue) and for TAg (red). Shown are representative epifluorescence pictures, with aberrant, uneven or fragmented nuclear morphology shown in zoomed-in boxes. Scale bar, 20 μm. (B and C) Bar graphs show the quantitation of uneven (B) and fragmented nuclei (C). In the infected samples, only the TAg-positive nuclei were scored. Each bar represents the average of the results from at least three independent experiments (an average of at least 80 nuclei were scored in each sample per independent experiment), and the error bars show the SD values. *, $P < 0.05$; **, $P < 0.01$.
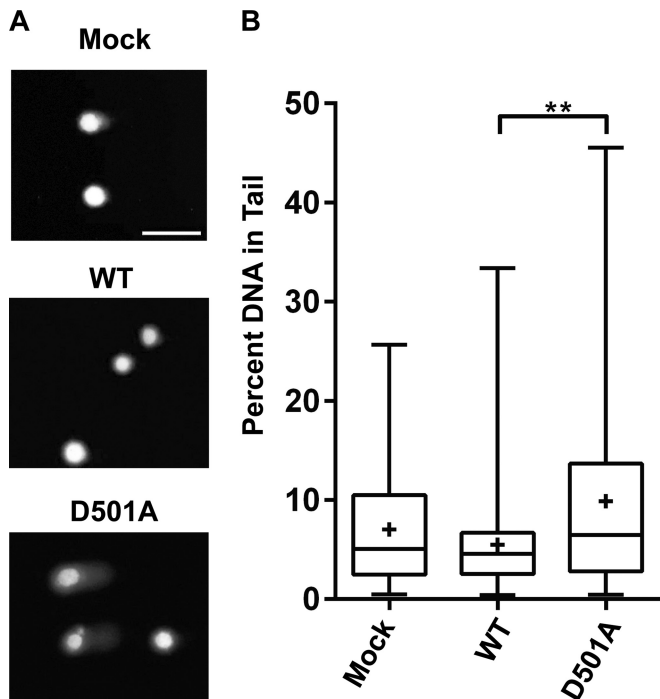
FIG 7 DNA damage accumulates in TAg D501A mutant virus-infected cells. An alkaline comet assay was used to determine host DNA damage. (A) Representative comet assay images of mock-infected cells (top) and cells infected with WT BKPyV (middle) and TAg D501A mutant virus (bottom). Scale bar, 100 μm. (B) Box-and-whisker plots demonstrating the distribution of DNA damage. Shown are combined results from three independent experiments. The top and bottom of the whiskers represent the maximum and minimum data points in the data set, respectively. The three horizontal lines of the boxes denote the first quartile, median, and third quartile, starting with the lowest line. The plus (+) sign in each plot is the average of the data. At least 50 events were scored per condition per experiment. **, $P < 0.01$.
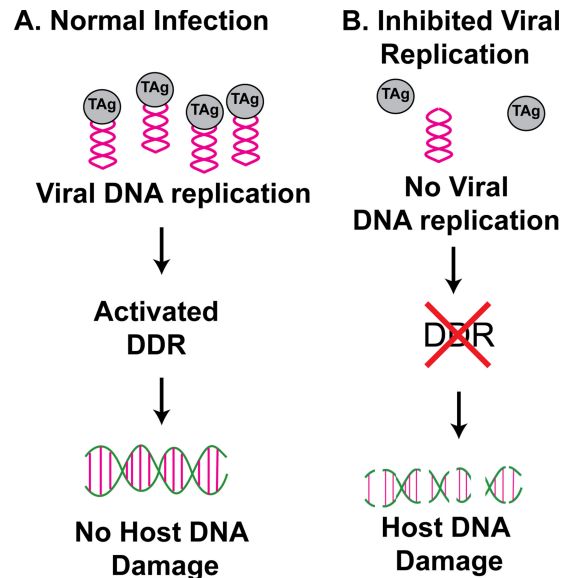

FIG 8 Model of DDR activation during BKPyV infection. BKPyV viral DNA replication activates both the ATM- and ATR-mediated DDRs in primary kidney epithelial cells. The activated DDR can, in turn, suppress the host DNA damage caused by polyomavirus infection. In the absence of viral DNA replication, host DDRs are not fully activated. The lack of DDR activation results in an accumulation of host DNA damage.

lication intermediates, as has been demonstrated for SV40 (6), but they may also have to rely on the activated DDR and subsequent cell cycle arrest to prevent detrimental events, such as mitotic catastrophe.

Our results with the D501A viral replication mutant strongly suggest that the activation of the DDR is dependent on viral replication. Although we cannot exclude the possibility that late events, such as late gene expression or virus packaging, may contribute to DDR activation, it is more likely that it is viral DNA replication that leads to a robust DDR activation. Similar conclusions have been made by Ellen Fanning's group during SV40 infection (6). How viral DNA replication results in the activation of the DDR remains to be further examined. Replication stress as a result of rapid viral replication could serve as a trigger for ATR activation. Recently, replication stress has also been linked to ATM activation in the absence of DNA damage under certain stress conditions (33). Alternatively, replication stress-induced replication fork collapse can lead to the generation of DSBs, which in turn activates the ATM branch of the DDR (34).

It is also interesting that the TAg D501A mutant can cause host DNA damage without triggering a strong DDR. It has been reported for mPyV that TAg can sensitize the cells to DNA-damaging conditions, such as UV or etoposide treatment (35). It is thought that this effect is caused by TAg binding to RPA and preventing RPA from localizing to repair foci following DNA damage. Similar sensitization to DNA damage has been observed with SV40 and JCPyV (36, 37). Therefore, in addition to a lack of viral DNA replication, another possible reason that the DDR is not activated during D501A mutant virus infection is that certain DDR signaling proteins are being sequestered by TAg. Future studies aimed toward understanding the molecular nature of the DNA damage caused by TAg, as well as identifying DDR binding partners for both wild-type and mutant TAgs, would provide more information on how DDR activation and DNA damage are affected by BKPyV infection.

In summary, we provide evidence here for a unique viral DNA replication-dependent DDR activation in primary cells infected with BKPyV, indicating an exquisite balance between virus-induced DDR activation and host genome stability. These findings showcase the extraordinary ability of polyomaviruses to orchestrate multiple host components to facilitate their replication and to suppress simultaneous damage to the host. Since polyomaviruses are a group of oncogenic viruses, our studies may also have implications in virus-induced genome instability and how that might be tied to viral replication status.

REFERENCES

1. **Bennett SM, Broekema NM, Imperiale MJ.** 2012. BK polyomavirus: emerging pathogen. Microbes Infect **14**:672–683. http://dx.doi.org/10.1016/j.micinf.2012.02.002.

2. **Egli A, Infanti L, Dumoulin A, Buser A, Samaridis J, Stebler C, Gosert R, Hirsch HH.** 2009. Prevalence of polyomavirus BK and JC infection and replication in 400 healthy blood donors. J Infect Dis **199**:837–846. http://dx.doi.org/10.1086/597126.

3. **Jiang M, Abend JR, Johnson SF, Imperiale MJ.** 2009. The role of polyomaviruses in human disease. Virology **384**:266–273. http://dx.doi.org/10.1016/j.virol.2008.09.027.

4. **Topalis D, Andrei G, Snoeck R.** 2013. The large tumor antigen: a "Swiss Army knife" protein possessing the functions required for the polyomavirus life cycle. Antiviral Res **97**:122–136. http://dx.doi.org/10.1016/j.antiviral.2012.11.007.

5. **Kitamura E, Blow JJ, Tanaka TU.** 2006. Live-cell imaging reveals replication of individual replicons in eukaryotic replication factories. Cell **125**:1297–1308. http://dx.doi.org/10.1016/j.cell.2006.04.041.

6. **Sowd GA, Li NY, Fanning E.** 2013. ATM and ATR activities maintain replication fork integrity during SV40 chromatin replication. PLoS Pathog **9**:e1003283. http://dx.doi.org/10.1371/journal.ppat.1003283.

7. **Zhao X, Madden-Fuentes RJ, Lou BX, Pipas JM, Gerhardt J, Rigell CJ, Fanning E.** 2008. Ataxia telangiectasia-mutated damage-signaling kinase- and proteasome-dependent destruction of Mre11-Rad50-Nbs1 subunits in simian virus 40-infected primate cells. J Virol **82**:5316–5328. http://dx.doi.org/10.1128/JVI.02677-07.

8. **Boichuk S, Hu L, Makielski K, Pandolfi PP, Gjoerup OV.** 2011. Functional connection between Rad51 and PML in homology-directed repair. PLoS One **6**:e25814. http://dx.doi.org/10.1371/journal.pone.0025814.

9. **Dahl J, You J, Benjamin TL.** 2005. Induction and utilization of an ATM signaling pathway by polyomavirus. J Virol **79**:13007–13017. http://dx.doi.org/10.1128/JVI.79.20.13007-13017.2005.

10. **Orba Y, Suzuki T, Makino Y, Kubota K, Tanaka S, Kimura T, Sawa H.** 2010. Large T antigen promotes JC virus replication in G2-arrested cells by inducing ATM- and ATR-mediated G2 checkpoint signaling. J Biol Chem **285**:1544–1554. http://dx.doi.org/10.1074/jbc.M109.064311.

11. **Tsang SH, Wang X, Li J, Buck CB, You J.** 2014. Host DNA damage response factors localize to Merkel cell polyomavirus DNA replication sites to support efficient viral DNA replication. J Virol **88**:3285–3297. http://dx.doi.org/10.1128/JVI.03656-13.

12. **Shi Y, Dodson GE, Shaikh S, Rundell K, Tibbetts RS.** 2005. Ataxia-telangiectasia-mutated (ATM) is a T-antigen kinase that controls SV40 viral replication in vivo. J Biol Chem **280**:40195–40200. http://dx.doi.org/10.1074/jbc.C500400200.

13. **Low J, Humes HD, Szczypka M, Imperiale M.** 2004. BKV and SV40 infection of human kidney tubular epithelial cells in vitro. Virology **323**:182–188. http://dx.doi.org/10.1016/j.virol.2004.03.027.

14. **Jiang M, Zhao L, Gamez M, Imperiale MJ.** 2012. Roles of ATM and ATR-mediated DNA damage responses during lytic BK polyomavirus infection. PLoS Pathog **8**:e1002898. http://dx.doi.org/10.1371/journal.ppat.1002898.

15. **Abend JR, Low JA, Imperiale MJ.** 2007. Inhibitory effect of gamma interferon on BK virus gene expression and replication. J Virol **81**:272–279. http://dx.doi.org/10.1128/JVI.01571-06.

16. **Jiang M, Abend JR, Tsai B, Imperiale MJ.** 2009. Early events during BK virus entry and disassembly. J Virol **83**:1350–1358. http://dx.doi.org/10.1128/JVI.02169-08.

17. **Broekema NM, Imperiale MJ.** 2012. Efficient propagation of archetype BK and JC polyomaviruses. Virology **422**:235–241. http://dx.doi.org/10.1016/j.virol.2011.10.026.

18. **Jiang M, Entezami P, Gamez M, Stamminger T, Imperiale MJ.** 2011. Functional reorganization of promyelocytic leukemia nuclear bodies during BK virus infection. mBio **2**(1):e00281-10. http://dx.doi.org/10.1128/mBio.00281-11.

19. **Broekema NM, Imperiale MJ.** 2013. miRNA regulation of BK polyomavirus replication during early infection. Proc Natl Acad Sci U S A **110**:8200–8205. http://dx.doi.org/10.1073/pnas.1301907110.

20. **Karen KA, Hoey PJ, Young CS, Hearing P.** 2009. Temporal regulation of the Mre11-Rad50-Nbs1 complex during adenovirus infection. J Virol **83**:4565–4573. http://dx.doi.org/10.1128/JVI.00042-09.

21. **Bakkenist CJ, Kastan MB.** 2003. DNA damage activates ATM through intermolecular autophosphorylation and dimer dissociation. Nature **421**:499–506. http://dx.doi.org/10.1038/nature01368.

22. **Kasahara K, Goto H, Enomoto M, Tomono Y, Kiyono T, Inagaki M.** 2010. 14-3-3gamma mediates Cdc25A proteolysis to block premature mitotic entry after DNA damage. EMBO J **29**:2802–2812. http://dx.doi.org/10.1038/emboj.2010.157.

23. **Reynisdottir I, Prives C.** 1992. Two conditional *tsA* mutant simian virus 40 T antigens display marked differences in thermal inactivation. J Virol **66**:6517–6526.

24. **Loeber G, Tevethia MJ, Schwedes JF, Tegtmeyer P.** 1989. Temperature-sensitive mutants identify crucial structural regions of simian virus 40 large T antigen. J Virol **63**:4426–4430.

25. **Hein J, Boichuk S, Wu J, Cheng Y, Freire R, Jat PS, Roberts TM, Gjoerup OV.** 2009. Simian virus 40 large T antigen disrupts genome integrity and activates a DNA damage response via Bub1 binding. J Virol **83**:117–127. http://dx.doi.org/10.1128/JVI.01515-08.

26. **Li J, Wang X, Diaz J, Tsang SH, Buck CB, You J.** 2013. Merkel cell polyomavirus large T antigen disrupts host genomic integrity and inhibits cellular proliferation. J Virol **87**:9173–9188. http://dx.doi.org/10.1128/JVI.01216-13.

27. **Jiao J, Simmons DT.** 2003. Nonspecific double-stranded DNA binding activity of simian virus 40 large T antigen is involved in melting and unwinding of the origin. J Virol **77**:12720–12728. http://dx.doi.org/10.1128/JVI.77.23.12720-12728.2003.

28. **Buck CB, Pastrana DV, Lowy DR, Schiller JT.** 2006. Generation of HPV pseudovirions using transfection and their use in neutralization assays. Methods Mol Med **119**:445–462. http://dx.doi.org/10.1385/1-59259-982-6:445.

29. **Mao Z, Bozzella M, Seluanov A, Gorbunova V.** 2008. DNA repair by nonhomologous end joining and homologous recombination during cell cycle in human cells. Cell Cycle **7**:2902–2906. http://dx.doi.org/10.4161/cc.7.18.6679.

30. **Abend JR, Joseph AE, Das D, Campbell-Cecen DB, Imperiale MJ.** 2009. A truncated T antigen expressed from an alternatively spliced BK virus early mRNA. J Gen Virol **90**:1238–1245. http://dx.doi.org/10.1099/vir.0.009159-0.

31. **Boichuk S, Hu L, Hein J, Gjoerup OV.** 2010. Multiple DNA damage signaling and repair pathways deregulated by simian virus 40 large T antigen. J Virol **84**:8007–8020. http://dx.doi.org/10.1128/JVI.00334-10.

32. **Hu L, Filippakis H, Huang H, Yen TJ, Gjoerup OV.** 2013. Replication stress and mitotic dysfunction in cells expressing simian virus 40 large T antigen. J Virol **87**:13179–13192. http://dx.doi.org/10.1128/JVI.02224-13.

33. **Olcina MM, Foskolou IP, Anbalagan S, Senra JM, Pires IM, Jiang Y, Ryan AJ, Hammond EM.** 2013. Replication stress and chromatin context link ATM activation to a role in DNA replication. Mol Cell **52**:758–766. http://dx.doi.org/10.1016/j.molcel.2013.10.019.

34. **Feng W, Di Rienzi SC, Raghuraman MK, Brewer BJ.** 2011. Replication stress-induced chromosome breakage is correlated with replication fork progression and is preceded by single-stranded DNA formation. G3 (Bethesda) **1**:327–335. http://dx.doi.org/10.1534/g3.111.000554.

35. **Banerjee P, DeJesus R, Gjoerup O, Schaffhausen BS.** 2013. Viral interference with DNA repair by targeting of the single-stranded DNA binding protein RPA. PLoS Pathog **9**:e1003725. http://dx.doi.org/10.1371/journal.ppat.1003725.

36. **Trojanek J, Ho T, Croul S, Wang JY, Chintapalli J, Koptyra M, Giordano A, Khalili K, Reiss K.** 2006. IRS-1-Rad51 nuclear interaction sensitizes JCV T-antigen positive medulloblastoma cells to genotoxic treatment. Int J Cancer **119**:539–548. http://dx.doi.org/10.1002/ijc.21828.

37. **Pietruska JR, Kane AB.** 2007. SV40 oncoproteins enhance asbestos-induced DNA double-strand breaks and abrogate senescence in murine mesothelial cells. Cancer Res **67**:3637–3645. http://dx.doi.org/10.1158/0008-5472.CAN-05-3727.